特集 電磁非破壊検査工学の体系化

Determining the sizes of 3-D surface cracks using dipole model of a crack and Hall element measurements

Dorian Minkov Tohoku University
Jinyi Lee Lacomm Co.,Ltd
Tetsuo Shoji Tohoku University

There is significant industrial demand for developing of faster methods for non-destructive inspection of surface cracks in metals. Our group has developed a method for estimating the sizes of surface cracks in magnetic materials based on dipole model of a crack. Hall voltage distributions are measured by Hall element sliding on the surface of the material along a line parallel to the direction of the applied magnetic field, perpendicular to the long axis of the crack, and halving its length. Surface cracks with different widths cut mechanically in SS400 steel specimens are investigated. Crack inversions are performed which show that the depth of the crack can be determined with 2 % error provided that the crack length and width are measured independently. When the crack width is unknown, the depth error is within 12 %, but the width error can be as large as 30 %.
Key Words : Surface crack, crack inversion, magnetic dipole, dipole model, magnetic material, hall voltage, Hall element, regression, RMS error.

1 Introduction

When magnetic field is applied inside a magnetic specimen, the magnetic field redistributes around a flaw, and a part of it named 'leakage magnetic field' leaves the specimen in the vicinity of the flaw. Correspondingly, magnetic methods represent a main tool for analyzing flaws and cracks (a crack is a flaw characterized by a very small width/depth ratio, and presence of a crack tip) in magnetic materials mostly as a result of their nondestructive essence and significant sensitivity. Static magnetic methods are especially attractive due to relatively large penetration depth of the field, simplicity of the experimental equipment, and the respective physical processes.

For example, pipeline inspection companies employ equipment called "pig" for internal constant magnetic field magnetization and measurement of flaw generated leakage magnetic field by Hall elements positioned at the inner wall of steel pipes. At this stage though they have not found satisfactory solution of the important problem for computing the sizes of such flaws (flaw inversion) [1,2]. Most approaches for flaw inversion based on static magnetic methods use analytical or semi-analytical solutions of the magnetic field distribution at every step of the inversion, which is computationally expensive. Besides, often simplified boundary conditions are utilized at the flaw walls, and volumetric material constants are employed instead of the required stress dependent material constants around the flaw [3,4].

Our group has developed a new approach for flaw inversion using the dipole model of a crack (DMC), static magnetization, and Hall element measurements [5,6]. The advantages of this approach are that it does not use analytical or semi-analytical solutions of the magnetic field distribution, neither imposing of predetermined boundary conditions at the crack walls, nor unknown and stress dependent material constants around the flaw.

Significant amount of work has been done on developing and adapting DMC to calculating intensity of leakage magnetic field (ILMF) of surface cracks in magnetic materials [7,8,9,10,11]. In all of these studies is assumed that the crack is filled homogeneously by magnetic dipoles, i.e. that the surface density of magnetic charge m has a constant value along the crack walls. It was shown in [12] though that this assumption leads to significant errors in calculating ILMF in the vicinity of different cracks which indicates that the distribution of magnetic dipoles along the crack depth should not be considered to be constant. Indeed, it can be expected that the larger intensity of magnetic field at the crack tip with respect to the crack mouth should be represented in DMC by employing larger value of m at the crack tip than at the crack mouth.

In this paper is presented analytical expression for the z-component of ILMF (ZILMF) of a right angular parallelepiped surface crack assuming linear depth distribution of m. This allows to calculate the Hall voltage distribution measured by a Hall element in the vicinity of a crack, and to perform inversion for determining the crack sizes. Steel specimens containing one machined artificial surface crack with right angular parallelepiped shape are investigated. Hall voltage distributions are measured by a Hall element sliding on the surface of the specimens along one measurement line which halves the crack length, and is parallel to the direction of the applied field, and perpendicular to the crack length. The crack depth and width are computed by a regression of such Hall voltage distribution.

2 Theory of the crack inversion

In DMC, a crack is represented as being filled by magnetic dipoles which are oriented in the same direction which is contrary to the direction of the applied magnetic field while the opposite dipole charges are located on the two opposite crack walls (Fig.1). A right-angular parallelepiped surface crack whose long axis y is perpendicular to the direction x of the applied filed,

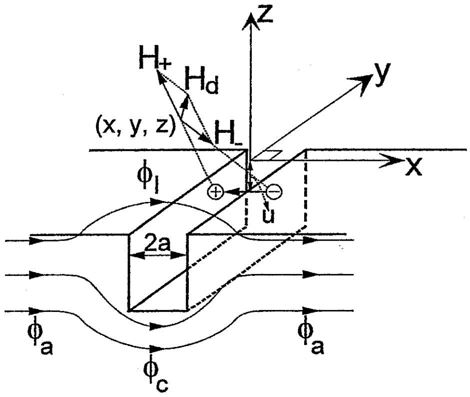

Fig. 1: Shematic representation of individual magnetic dipole in DMC, its ILMF H_d, and distribution of magnetic flux Φ around the crack.

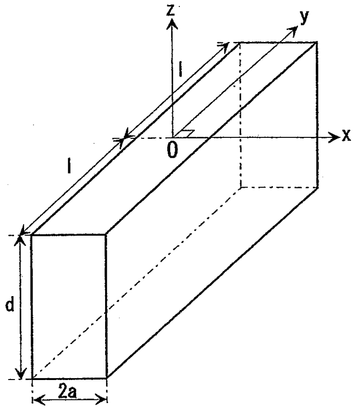

Fig. 2: Right-angular parallelepiped surface crack. The applied magnetic field is directed along the x axis, and (x0y) is the surface plane of the specimen.

and which has length 2l, width 2a, and depth d is illustrated in Fig.2. According to [13], ZILMF of this crack is represented by integrating ZILMF of all of the dipoles filling the crack:

$$H_z(x,y,z) = \int_{-l}^{l-y}\int_{0}^{d} \frac{m(u)}{4\pi\mu_0} \left\{ \frac{(z+u)(du)(dy)}{\left[(x+a)^2+y^2+(z+u)^2\right]^{3/2}} \right. ,$$

$$= \left. - \frac{(z+u)(du)(dy)}{\left[(x+a)^2+y^2+(z+u)^2\right]^{3/2}} \right\} \qquad (1)$$

where $(l-y)(x-a)$ m is the surface density of magnetic charge at the crack walls.

The distribution of m along the crack depth is considered to be linear:

$$m(u)|_{u\subset[0,d]} = m(v)|_{v=u/d\subset[0,1]} = m_1 + m_2 \qquad (2)$$

while at the crack mouth $m(0)|_{u=0} = m_1$, and the slope of this distribution is m_2.

The integration in Eq. (1) gives the following analytical expression for ZILMF of a right-angular parallelepiped surface crack with linear depth distribution of m:

$$
\begin{aligned}
H_z(x,y,z) &= w_1 \left[\begin{array}{c} A_1(l-y,x+a)+A_1(l+y,x+a) \\ -A_1(l-y,x-a)-A_1(l+y,x-a) \end{array} \right] \\
&- w_2 \left[A_2(l-y,x+a)+A_2(l+y,x+a) \right] \\
&+ w_3 \left[A_2(l-y,x-a)+A_2(l+y,x-a) \right] \\
&+ w_4 \left[\begin{array}{c} A_3(l-y,x+a)+A_3(l+y,x+a) \\ -A_3(l-y,x-a)-A_3(l+y,x-a) \end{array} \right]
\end{aligned} \tag{3}
$$

where

$$
\begin{aligned}
w_1 &= (m_1 - m_2 z/d)/(4\pi\mu_0) \quad , \\
w_2 &= (x+a)^2 m_2/(4\pi\mu_0 d) \quad , \\
w_3 &= (x-a)^2/(4\pi\mu_0 d) \quad , w_4 = m_2/(4\pi\mu_0 d),
\end{aligned}
$$

$$
A_1(l-y,x-a) = ln\left[\sqrt{\frac{(x-a)^2+(z+d)^2}{(x-a)^2+z^2}} \cdot \frac{(l-y)+\sqrt{(x-a)^2+(l-y)^2+z^2}}{(l-y)+\sqrt{(x-a)^2+(l-y)^2+(z+d)^2}}\right]
$$

$$
A_2(l-y,x-a) = \frac{1}{x-a}\tan^{-1}[A_{21}(l-y,x-a)]
$$

$$
A_{21}(l-y,x-a) = \frac{(l-y)(x-a)(z+d)\sqrt{(x-a)^2+(l-y)^2+z^2}}{A_{22}(x-a)^2\sqrt{(x-a)^2+(l-y)^2+z^2}} - \frac{(l-y)(x-a)z\sqrt{(x-a)^2+(l-y)^2+(z+d)^2}}{A_{22}(x-a)^2\sqrt{(x-a)^2+(l-y)^2+z^2}}
$$

$$
A(l-y,x-a) = \sqrt{(x-a)^2+(l-y)^2+(z+d)^2+(l-y)^2 z(z+d)}
$$

$$
A_3(l-y,x-a) = (l-y)ln\left[\frac{\sqrt{(x-a)^2+(l-y)^2+(z+d)^2}+z+d}{\sqrt{(x-a)^2+(l-y)^2+z^2}+z}\right]
$$

and $A_i(l-y,x+a)$, $A_i(l+y,x-a)$, and $A_i(l+y,x+a)$ for $i = 1 \div 3$ are obtained by replacing respectively $x-a$ by $x+a$, $l-y$ by $l+y$, and both $l-y$ by $l+y$ and $x-a$ by $x+a$ in the above expressions for $A_i(l-y,x-a)$.

The Hall voltage measured by a Hall element located on the surface of the investigated specimen represents a measure of ZILMF. Taking into account that in most cases both the length of the semiconductor chip of the Hall element and the crack width are of the order of several hundred micrometers, ZILMF can vary significantly over the surface of the chip. Correspondingly, it was proven in [6] that the measured Hall voltage is proportional to average value of ZILMF over the volume of the active layer of the chip:

$$
V_H = \frac{\mu_0 I}{qnd_a}\frac{\sum_{i_1=1}^{N_1}\sum_{i_2=1}^{N_1}\sum_{i_3=1}^{N_2} H_{i_1,i_2,i_3}}{{N_1}^2 N_2} = \frac{\mu_0 I}{qnd_a}H_a = cH_a, \tag{4}
$$

where I is the electric current applied between two opposite contacts of the Hall element, V_H is the Hall voltage measured between the other two opposite contacts, d_a is the thickness of the active layer of the chip, μ_0 is the vacuum permeability, q is the absolute value of the electron charge, n is the electron concentration in the active layer which is assumed to be n-type and to have square shaped surface, the volume of the active layer is represented as a sum of its constituent parallelepipeds, N_1 and N_2 are the numbers of such constituent parallelepipeds along the length and the thickness of the active layer, H_{i_1,i_2,i_3} is the z-component of the intensity of the leakage magnetic field $Hz(x,y,z)$ in the center of the constituent parallelepiped with number i_1,i_2,i_3, H_a is the average value of ZILMF over the volume of the active layer, and $c = \mu_0 I/qnd_a$ is a constant.

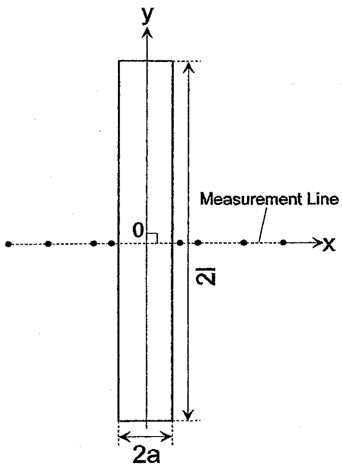

Fig. 3: Surface view of an investigated crack. Measurement pointw (•) of the Hall voltage are located slong the measurement line (- - -).

Hall voltages are measured in several points of orthogonal projections of the geometrical centre of the active layer onto the specimen's surface which are located along a measurement line

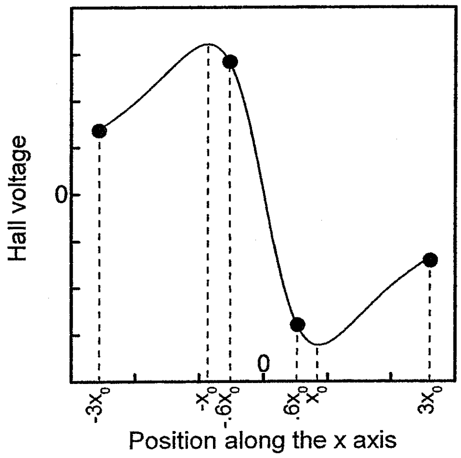

Fig. 4: Theoretical Hall voltage distribution along the measurement line, and positioning of the measurement intervals [-3x_0, -0.6x_0], and [0.6x_0, 3x_0].

parallel to the direction x of the applied field, perpendicular to the long axis y of the crack, and passing through the centre 0 of the investigated crack (Fig.3). The measurement distance between the centre of the active layer of the chip and the surface of the specimen is designated by z_m. The distributions along the measurement line of both ZILMF and the Hall voltage are anti-symmetrical with respect to the crack centre 0, i.e. $H_z(x,y,z) = -Hz(-x,y,z)$, and $V_H(x,y,z) = -V_H(-x,y,z)$ (Eqs. (1), and (4)). Respectively, the measurement points can be chosen to be positioned on the same side of the long axis y of the crack. The locations of the measurement points are selected to provide maximum information about the distribution of the Hall voltage along the measurement line, and the number N of measurement points is kept relatively small. Correspondingly, all of the measurement points are located along the measurement line and are positioned within the interval [-3x_0, -0.6x_0] or/and the interval [0.6x_0, 3x_0] from the centre 0 of the investigated crack where x_0 is the distance between the crack centre and the location of the minimum value of the Hall voltage along the measurement line (Fig. 4).

The Hall voltage values in the measurement points depend on the geometrical sizes of the crack, and the distribution of m along the crack depth. The unknown crack sizes and the depth distribution of m can be determined by a regression for the Hall voltage distribution which reduces to minimising the root mean square error $RMS = \sqrt{\left\{\sum_{i=1}^{N}\left[V_H^m(i) - V_H^t(i)\right]^2\right\}/N}$ between the measured distribution $V_H^m(i)$ and the theoretical distribution $V_H^t(i)$ of the Hall voltage for the N measurement points. This provides computer predicted values of the above unknown parameters which give a new theoretical distribution $V_H^t(i)$ at every step of the minimisation while the RMS error decreases. The RMS error is minimised using the Nelder-Meade simplex search [14], and the minimisation procedure ends when the RMS error reaches saturation.

It was shown in [15], based on a comparison between measured and theoretical Hall voltage distributions of different surface cracks, that m has larger value at the crack tip with respect to the crack mouth, i.e. $m_1 \geq 0$, and $m_2 \geq 0$, and the slope m_2 of the linear depth distribution of m is limited within the following interval:

$$0.26 \leq m_2 \leq 0.99 \tag{5}$$

for surface cracks in SS400 steel specimens magnetised by a magnetic coil supplied by 3A DC current, and Hall voltages measured by THS124 Hall element with active region sizes $l_a \times l_a \times d_a = 125 \times 125 \times 6\mu m$ supplied by DC current $I = 5$ mA.

3 Results

Two right-angular parallelepiped specimens of SS400 steel with dimensions $200 \times 10 \times 5$ mm are utilised in this study. One right-angular surface crack is cut mechanically in the middle of the length of each one of the specimens and along its entire width, i.e. the crack length is $2l = 10$ mm. One of the specimens contains a crack with width $2a = 0.7$ mm, and the other- a crack with width $2a = 0.9$ mm while the depths of both of these cracks are $d = 3$ mm. Two magnetic coils wound around the specimen are used for applying magnetic field.

Hall voltage distributions are measured by Toshiba THS124 GaAs Hall element supplied by DC current $I = 5$ mA, which leads to $c = 2.096*10^{-6}$ $\Omega.m$ in Eq. (4). The sizes of the active region of the semiconductor chip of THS124 are $l_a \times l_a d_a = 125 \times 125 \times 6\mu m$. The top square planar surface of the plastic encapsulation of the Hall element is positioned onto the surface of the specimen, and the centre of this surface can move along the measurement line during the Hall voltage measurements. This setup is illustrated in Fig. 5, and it results in measurement distance $z_m = 0.54$ mm between the surface of the specimen and the centre of the active layer of the chip. The Hall element is moved manually by non-magnetic plastic precise positioning equipment.

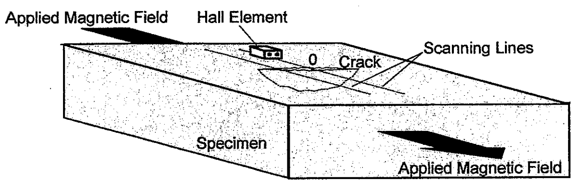

Fig. 5: Illustration of the Hall voltage distribution measurement setup. The top surface of the Hall element is positioned onto the specimen's surface, and can move along the measurement line.

The measured Hall voltage distribution, for an investigated crack, is determined by two sets of Hall voltage measurements which are performed at the same fourteen points located equidistantly with a step of 0.1 mm within the interval [$-3x_0$, $-0.6x_0$] or/and the interval [$0.6x_0$, $3x_0$] along the measurement line- the first set is for magnetising DC current $I_a = 0$ A and the second set is for magnetising DC current $I_a = 3$ A supplied to both magnetic coils. The measured Hall voltage distribution used in the computations represents a difference between the Hall voltages for Ia=3 A and Ia=0 A for each one of the measurement points. This measurement approach allows discounting the influence of residual magnetic fields due to residual magnetisation, external magnetic fields, etc.

The experimental conditions are described by introducing Case symbols. The first symbol is chosen to be 1 for the specimen containing crack with width 0.7 mm, and 2 for the crack with width 0.9 mm. The second symbol is 1 for the positive branch of the Hall voltage distribution characterised by $V_H > 0$, and 2 for the negative branch with $V_H < 0$. For example, the symbol 22 means that the specimen containing crack with width 0.9 mm is investigated, and only the negative branch is used in the inversion. The measured distribution of the Hall voltage along the measurement line is shown in Fig. 6 for the specimen containing the crack with width 0.7 mm.

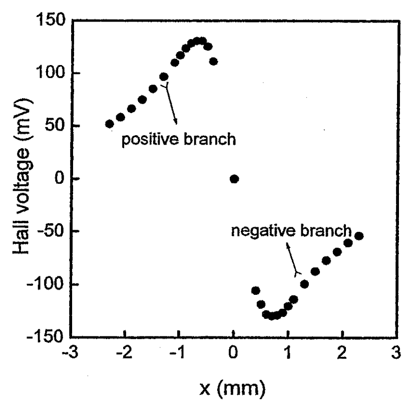

Fig. 6: Experimental Hall voltage distribution along the measurement line for the specimen containing crack with width 0.7 mm

Crack inversions are realised based on Eqs. (1-5), i.e. using linear depth distribution of m with limited slope, with $N_1 = 10$ and $N_2 = 1$ in Eq. (4). It is assumed in the computations that: it is known that the investigated cracks have right angular parallelepiped shape, and the crack length 2l is measured independently i.e. l is also known. Some crack inversions are per-

Table 1: Computed values of the unknown inversion parameters, crack depth error $|d_{tr} - d|/d_{tr}$,and RMS error when the crack width is known. Only the positive or the negatice branch of the measured Hall voltage distribution is used when computing the first four raws of parameters, and both brranches are used for the last two raws.

Case Symbol	m_1 $[H.A/m^2]$	m_2 $[H.A/m^2]$	d (mm)	$\|d_{tr} - d\|/d_{tr}$ (%)	RMS Error (mV)
11	0.713	0.260	3.041	1.4	0.52
12	0.728	0.26	3.235	7.8	0.84
21	0.548	0.836	2.667	11.1	1.10
22	0.491	0.990	2.962	1.3	0.73
11+12	0.721	0.260	3.111	3.7	1.50
21+22	0.524	0.990	2.802	6.6	2.50

Table 2: Computed values of the unknown crack parameters, crack width erroe, crack depth error, and RMS error when the crack width is unknown. $2A_{tr}$ and d_{tr} are the 'true values' of the crack width and depth

Case Symbol	a (mm)	d (mm)	$\|a_{tr} - a\|/a_{tr}$ (%)	$\|d_{tr} - d\|/d_{tr}$ (%)	RMS Error (mV)
11	0.262	3.329	25.1	11.0	0.36
22	0.583	2.776	29.6	7.5	0.64

formed with respect to the unknown parameters m_1, m_2, and d for the two specimens employing different Hall voltage distributions, assuming that the crack width 2a is measured independently. The results are presented in Table 1. Another crack inversions are performed for unknown crack width, i.e. for minimisation parameters m_1, m_2, a, and d. These results are given in Table 2.

4 Discussion

The data from Table 1 illustrate that both m1 and m2 have always positive values. This is consistent with the fact that the intensity of magnetic field at the crack tip is larger than at the crack mouth, which is represented in DMC by employing larger surface density of magnetic charge m at the crack tip with respect to the crack mouth. Furthermore, the crack depth error $|d_{tr} - d|/d_{tr}$ does not exceed 12 % when the crack width is known. It is also seen that for the crack with width $2a = 0.7$ mm, the RMS error is smaller for Case symbol 11 than for Case symbol 12, i.e. when the positive branch of the Hall voltage distribution is utilised rather than its negative branch.

This indicates that the inversion for the crack with width 0.7 mm is more accurate when using the positive branch (Case symbol 11) rather than the negative branch (Case symbol 12). The reason for this is the larger accuracy of the measured Hall voltage distribution for the positive branch with respect to the negative branch of the investigated crack. Similarly, the inversion for the crack with width 0.9 mm is more accurate if the negative branch (Case symbol 22) is employed rather than the positive branch (Case symbol 21). Table 1 shows that the depth error does not exceed 2 % for Case symbols 11 and 22.

Correspondingly, utilisation of the branch of the Hall voltage distribution which provides smaller RMS error leads to decreasing the depth error.

When both the negative and the positive branch of the Hall voltage distribution are used in the crack inversion, the depth error does not exceed 7 %, according to the last two rows of Table 1, and its value is in between the depth errors for the corresponding positive and negative branches. The relatively large value of the depth error in this case is due to employing the less accurately measured branch (the negative branch for the crack with width 0.7 mm, and the positive branch for the crack with width 0.9 mm).

It is seen from Table 2 that, if both the width and the depth of the crack are unknown, the depth error does not exceed 12 % while the width error does not exceed 30 % provided that the more accurate branch of the Hall voltage distribution is used. This is an indication that the width error might be inadmissibly large when the Hall voltage distribution is measured by our present technology.

It can be speculated though that the accuracy of both the measured Hall voltage distribution, and the crack inversion can be increased by employing InSb or InAs Hall elements which are characterised by improved linearity, and reproducibility of their VH(H) dependencies over time with respect to the GaAs Hall elements utilised in the present study [16], as well as by more precise determining the location of the Hall element based on machine position control, and ensuring higher temperature stability during the experiment. Furthermore, the presented crack inversion method could be used for determining effective depth and effective width of real cracks which would be of interest e.g. for pipeline inspection.

Acknowledgments

This work was supported by Grant-in Aid for Centre of Excellence Research No. 11CE2003 of the Japanese Ministry of Education, Science, Sports, and Culture. The authors would like also to thank Dr. Y.Sato for his technical assistance.

参考文献

[1] J.H.J. Stalenhoef and J.A. de Raad, MFL and PEC Tools for Plant Inspection, *Proceedings of the 7th ECNDT*, (1998), pp.1831-1837.

[2] S.A. Mandayam and J.L. Schmalzel, Compensation Techniques for Magnetic Flux Leakage Indications in X-Grade Gas Transmission Pipelines - Experimental Results, *Short papers of the 5th ENDE*, (1999), p.10.

[3] W. Lord, Computer Simulation of Electromagnetics NDT Phenomena - A Personal Perspective, *Short papers of the 5th ENDE*, (1999), pp.2-3.

[4] J.R. Bowler and N. Harfield, Magnetic Field Evaluation for Application to Magnetic Particle Inspection, *Short papers of the 5th ENDE*, (1999), pp.5-6.

[5] D. Minkov and T. Shoji, Method for Sizing of 3-D Surface Breaking Flaws by Leakage Flux, *NDT&E International*, 31 (1998), pp.317-324.

[6] D. Minkov and T. Shoji, Sizing of 3-D Surface Cracks by Using Hall Element Probe, *Electromagnetic Nondestructive Evaluation (III)*, IOS Press, (1999), pp.283-291.

[7] N.N. Zatsepin and V.E. Scherbinin, Calculation of the Magnetostatic Field of Surface Defects, *Defektoskopiya*, 2 (1966), pp.385-399.

[8] G. Dobbman and P. Holler, Physical Analysis Method of Magnetic Flux Leakage, *Research Techniques in Nondestructive Testing*, Academic Press, (1980), pp.39-69.

[9] I. Uetake and H. Ito, Lift-Off Effect on Magnetic Leakage Flux Method and Its Application to Defect Size Estimation, *Nondestructive Inspection*, 33 (1984), pp.788-797.

[10] C. Edwards and S.B. Palmer, Simulation of the Effects of Current Leakage Across Thin Cracks, *J. Phys. D: Appl. Phys.*, 19 (1986), pp.657-663.

[11] F. Forster, New Findings in the Field of Non-Destructive Magnetic Leakage Field Inspection, *NDT International*, 19 (1986), pp.3-14.

[12] D. Minkov, J. Lee and T. Shoji, Experimental study of sizing of surface cracks by using leakage magnetic field and Hall element probe, *Abstracts of the 2th International Conference 'Emerging Technologies in NDT'*, (1999), pp.7-8.

[13] S. Mukae, M. Katoh and K. Nishio, Investigation on Quantitization of Defect and Effect of Factors Affecting Leakage Flux Density in Magnetic Leakage Flux Testing Method, *NDT Inspection*, 37 (1988), pp.885-893.

[14] J.J. Dennis and D.J. Woods, New Computing Environments; Microcomputers in Large-Scale Computing, *SIAM*, (1987), pp.210-218.

[15] D. Minkov and T. Shoji, Study of the Dipole Model of a Crack, *Abstracts of Quantitative NDE'99*, (1999), p.82.

[16] Asahi Kasei Electronics, Asahi Hall Elements Catalogue, (1999), pp.18-38.